JOURNAL OF AGRICULTURAL AND FOOD CHEMISTRY

Article

pubs.acs.org/JAFC

Improvement of *Alcaligenes faecalis* Nitrilase by Gene Site Saturation Mutagenesis and Its Application in Stereospecific Biosynthesis of (*R*)-(−)-Mandelic Acid

Zhi-Qiang Liu,[†] Xin-Hong Zhang,[†] Ya-Ping Xue,[†] Ming Xu,[‡] and Yu-Guo Zheng*[,†]

[†]Institute of Bioengineering, Zhejiang University of Technology, Hangzhou, Zhejiang 310014, People's Republic of China

[‡]Zhejiang Laiyi Biotechnology Co., Ltd, Shengzhou, Zhejiang 312400, People's Republic of China

Supporting Information

ABSTRACT: Nitrilases have recently received considerable attention as the biocatalysts for stereospecific production of carboxylic acids. To improve the activity, the nitrilase from *Alcaligenes faecalis* was selected for further modification by the gene site saturation mutagenesis method (GSSM), based on homology modeling and previous reports about mutations. After mutagenesis, the positive mutants were selected using a convenient two-step high-throughput screening method based on product formation and pH indicator combined with the HPLC method. After three rounds of GSSM, Mut3 (Gln196Ser/Ala284Ile) with the highest activity and ability of tolerance to the substrate was selected. As compared to the wild-type *A. faecalis* nitrilase, Mut3 showed 154% higher specific activity. Mut3 could retain 91.6% of its residual activity after incubation at pH 6.5 for 6 h. In a fed-batch reaction with 800 mM mandelonitrile as the substrate, the cumulative production of (*R*)-(−)-mandelic acid after 7.5 h of conversion reached 693 mM with an enantiomeric excess of 99%, and the space-time productivity of Mut3 was 21.50-fold higher than that of wild-type nitrilase. The K_m, V_{max}, and k_{cat} of wild-type and Mut3 for mandelonitrile were 20.64 mM, 33.74 μmol mg^{-1} min^{-1}, 24.45 s^{-1}, and 9.24 mM, 47.68 μmol mg^{-1} min^{-1}, and 34.55 s^{-1}, respectively. A homology modeling and molecular docking study showed that the diameter of the catalytic tunnel of Mut3 became longer and that the tunnel volume was smaller. These structural changes are proposed to improve the hydrolytic activity and pH stability of Mut3. Mut3 has the potential for industrial applications in the upscale production of (*R*)-(−)-mandelic acid.

KEYWORDS: *nitrilase, molecular modification, gene site saturation mutagenesis, mandelonitrile, (R)-(−)-mandelic acid*

INTRODUCTION

Nitrilases (EC 3.5.5.1) are important industrial enzymes used to convert nitriles directly into corresponding carboxylic acids and ammonia in a single step with mild conditions.[1,2] Occurrences, catalytic mechanisms, applicabilities, and molecular modifications of nitrilases have been widely reported.[3−5] By far, all known nitrilases can be classified as aromatic nitrilases, aliphatic nitrilases, and arylacetonitrilases according to substrate specificity.[6] Nitrilases are found in many plants and microorganisms, and their applications have been widely explored.[6] Recently, screening new nitrilases, exploring their applications, and the molecular modification of nitrilases are becoming hot issues because of the important application of nitrilases.[4,5,7−10]

It was reported that one of the important industrial applications of nitrilases is the conversion of (*R*,*S*)-mandelonitrile to (*R*)-(−)-mandelic acid.[11] This reaction exhibits excellent enantioselectivity, low-cost starting material, and most especially the possibility of performing a dynamic kinetic resolution of racemic substrate which provides theoretically 100% yield of the product.[11,12] (*R*)-(−)-mandelic acid has been used as an important intermediate for the production of pharmaceuticals such as semisynthetic penicillins, cephalosporins, antitumor agents, antiobesity agents, and chiral resolving agent for the resolution of racemic alcohols and amines.[12,13] (*R*)-(−)-mandelic acid can be produced by two routes including chemical and biosynthetic methods.[14] Biocatalytic synthesis of (*R*)-(−)-mandelic acid has been widespread because of its industrial development and application prospects.[11,12,15,16] The production of (*R*)-(−)-mandelic acid by nitrilases has the most potential for the industrial application.[11,15,17] There are several reported strains with abilities for the bioproduction of (*R*)-(−)-mandelic acid, including *Alcaligenes* sp. ECU0401,[18] *Pseudomonas putida* MTCC 5110[7,19] *A. faecalis* ZJUTB10,[5,11] *A. faecalis* ATCC 8750,[20] *P. fluorescens* EBC191,[8] *A. faecalis* JM3,[21] *Bradyrhizobium japonicum* USDA110,[22] and *Burkholderia cenocepacia* J2315.[23] However, the reported nitrilases still cannot meet the requirement for the industrial production of (*R*)-(−)-mandelic acid because of their poor activity and lower stability under low pH. To resolve this problem, nitrilases from different origins have been modified by various approaches.[3,5,24]

The gene site saturation mutagenesis method (GSSM) is widely used in the modification of proteins based on the PCR method, which has made a series of high-profile achievements on nitrilases.[25] Yeom et al. had mentioned that a positively charged amino acid at position 129 in nitrilase from *Rhodococcus rhodochrous* ATCC 33278 was an essential residue for the activity with meta-substituted benzonitriles by the

Received: December 24, 2013
Revised: March 29, 2014
Accepted: April 27, 2014
Published: April 28, 2014

GSSM.[26] Wu et al. obtained a mutant nitrilase with increased activity, specificity, and stability by modification at sites Thr210 and Leu201 located in α6, and Phe168 at the junction of the β10 helix and α6.[27,28] Nolan et al. found that the active sites for cyanide hydratase and nitrilase activity in the protein were the same by the GSSM.[29] The cyanide dihydratase completely lost its activity by the replacement of Cys163 to Ser, and the replacement of Tyr53 to Phe caused an increase of the K_m value of the enzyme for cyanide when the conserved amino acid residues in the cyanide dihydratase from *P. stutzeri* AK61 were altered by GSSM.[30]

In this study, the recombinant nitrilase from *A. faecalis* was selected to improve activity by using GSSM. On the basis of the secondary and three-dimensional structures, interactions between the substrate and nitrilase, and previous reports,[5,31,32] three sites in the α-helix (Leu175, Ala197, and Val305) and one site in the β-sheet (Ala284) located after Cys163 were selected for further mutagenesis. The site Gln196 was also selected using the software HotSpot Wizard to identify the point that plays an important role in enzyme catalysis and substrate specificity. After mutagenesis, the mutants were screened by a two-step screening method based on bromocresol purple as the pH indicator combined with liquid chromatography, and the best mutant Mut3 with serendipitously improved activity and pH stability was obtained. The characteristics of purified wild-type and Mut3 were studied and compared. The homology modeling and molecular docking were further studied to elucidate the interactions between substrate and nitrilase. Finally, the potential application in the kinetic resolution of racemic mandelonitrile to prepare *R*-(−)-mandelic acid was evaluated as well.

MATERIALS AND METHODS

Strains, Plasmids, and Medium. *E. coli* BL21 (DE3) (F-ompT gal dcm lon, hsdSB (rB- mB-) λ (DE3 (lacI lacUV5-T7 gene 1 ind1 sam7 nin5))) (Invitrogen, Karlsruhe, Germany) was used for heterologous expression. *E. coli* and recombinant *E. coli* strains were grown in Luria−Bertani (LB) medium (tryptone 10 g/L, yeast extract 5 g/L, and NaCl 10 g/L). The pET28b-NIT plasmid and recombinant nitrilase from *A. faecalis* was constructed and stored in our laboratory.[5] *Dpn* I and PrimeSTAR HS DNA polymerase were provided by the TaKaRa company (Dalian, China). (*R*,*S*)-mandelonitrile, (*R*)-(−)-mandelic acid, and (*S*)-(−)-mandelic acid were purchased from Sigma (St. Louis, MO). All other reagents and chemicals were commercially available and of analytic grade.

Table 1. Primers for the Gene Site Saturation Mutagenesis

positions of mutant	primers
Leu175	L175 (F): 5′-CTCTGTACTCCGAANNNGCGCACGCTCTGTC-3′
	L175 (R): 5′-GACAGAGCGTGCGCNNNTTCGGAGTACAGAG-3′
Ala197	A197 (F): 5′-CTGTACTCCGAACAGNNNCACGCTCTGTC-3′
	A197 (R): 5′-CAGAGCGTGNNNCTGTTCGGAGTACAGAGA-3′
Val305	V305 (F): 5′-GTCTAAATACGCCNNNTACTCCCAGCACGAAG-3′
	V305 (R): 5′-CTTCGTGCTGGGAGTANNNGGCGTATTTAGAC-3′
Ala284	A284 (F): 5′-GAAGCCACTCGTCTGNNNCTGGATCTGGGTC-3′
	A284 (R): 5′-GACCCAGATCCAGNNNCAGACGAGTGGCTTC-3′
Gln196	Q196 (F): 5′-CATGGAAGAGATCNNNTTCGCTAAGGCTATC-3′
	Q196 (R): 5′-GATAGCCTTAGCGAANNNGATCTCTTCCATG-3′

Gene Site Saturation Mutagenesis. Random mutations were introduced to the nitrilase gene by GSSM at positions of Leu175, Ala197, Val305, Ala284, and Gln196 using PrimeSTAR HS DNA polymerase (Takara) and pET28b-NIT plasmid as a template. The five pairs of primers carrying mutations are listed in Table 1. The plasmids with positive mutations from the previous round of mutations were used as a template for the next step of mutation. The PCR reaction mixture consisted of 200 μM for each dNTP, 0.2 μM primers, 10 μL of 5× PrimeSTAR Buffer (Mg^{2+} plus), and 1.25 U PrimeSTAR HS DNA polymerase (Takara) in 50 μL. The reaction was carried out at 94 °C for 5 min, followed by 30 cycles of 98 °C for 10 s, 55 °C for 15 s for amplifying the nitrilase gene, 72 °C for 8 min, and then 72 °C for 10 min in a PCR thermocycler (Biometra, Göttingen, Germany). PCR products were subjected to 0.9% agarose electrophoresis and then purified by a PCR purification kit (Simgen, Hangzhou, China). After purification, the DNA fragment was digested with *Dpn* I at 37 °C for 3 h to remove the template plasmid containing the methylation sites. The plasmid pET28b-NIT_{mut} was then transformed into *E. coli* BL21 (DE3) by the heat-shock method.[33]

Screening Method. A two-step screening method which was constructed to screen the mutants was described below: Each single colony was picked from the plate with 50 mg/mL kanamycin (Kan) to 96-well plates with LB broth and incubated overnight with vigorous shaking (500 rpm) at 37 °C. One part of the culture was transferred to the new 96-well plates with 50 mg/mL Kan, 0.1 mM isopropyl-β-D-thiogalactoside (IPTG), 100 mM (*R*,*S*)-mandelonitrile, and LB medium, and then thermomixed for 8−10 h at 30 °C. (*R*,*S*)-Mandelonitrile would be catalyzed to (*R*)-(−)-mandelic acid by nitrilase expressed by IPTG induction. The final concentration of 0.01% (w/v) bromocresol purple solution was added for high-throughput and rapid screening. The pH of the medium in the 96-well plate was kept at 7.0, and the screening method was based on the formation of yellow caused by mandelic acid as a result of hydrolysis by positive mutants. When the pH became lower and lower with the hydrolysis process of the (*R*,*S*)-mandelonitrile to produce mandelic acid, the medium with purple background would change the color to yellow. Finally, the positive mutants were selected by the formation of yellow. At the same time, the mutants which made the color of bromocresol purple solution change from purple to yellow were picked from the corresponding plates and grown at 37 °C in 50 mL of LB media containing 50 μL of 50 mg/mL Kan for further tests. The nitrilase was induced by the addition of 0.1 mM IPTG when optical density (OD) at 600 nm of the culture broth reached between 0.6 and 0.8. The cells were then incubated at 28 °C for 12 h and harvested by centrifugation at 9000 rpm for 10 min. The reaction was carried out with free cells in 1 mL of pure water at 40 °C, 500 rpm for 10 min. After reaction, the reaction mixture was centrifuged at 12000 rpm for 5 min, and then the amount of (*R*)-(−)-mandelic acid in the supernatant was subsequently determined by high-performance liquid chromatography (HPLC) mentioned below to further confirm the positive mutants with improved nitrilase activity.

Nitrilase Purification and Sodium Dodecyl Dulfate−Polyacrylamide Gel Electrophoresis (SDS−PAGE). After being induced by 0.1 mM IPTG, the cells harboring recombinant nitrilases were collected by centrifugation and then were resuspended in 30 mL of pure water and lysed by sonication with a Vibra-Cell VC 505 ultrasonic processor (Sonics and Materials Inc., Newtown, CT) at 400 W for 15 min. The resulting slurry was centrifuged at 12000 rpm for 20 min, and the supernatant was loaded to a nickel-NTA superflow column, which has been equilibrated with buffer (20 mM NaH_2PO_4 and 300 mM NaCl; and pH 8.0). Unbound proteins were washed out from the column with buffer (20 mM NaH_2PO_4, 300 mM NaCl, 50 mM imidazole, and pH 8.0). The active enzyme was eluted with buffer by a linear gradient from 50 to 500 mM imidazole at a flow rate of 1 mL/min. The purified enzymes were analyzed using 12% SDS−PAGE.

Enzyme Assays and Protein Assay. The standard activity assay was carried out using (*R*,*S*)-mandelonitrile (100 mM) as substrate and 0.2 mg/mL of purified enzyme mixed in potassium phosphate buffer (100 mM and pH 8.0). The reaction mixture (total volume 10 mL) was incubated at 45 °C for 10 min and stopped by HCl solution (final 2 M). Then, 200 μL of the mixture was centrifuged at 12000 rpm for 20 min, and the supernatant was subjected to HPLC analysis as described below for assaying the nitrilase activity. The amount of (*R*)-(−)-mandelic acid was determined by a LC-20AD prominence liquid chromatography instrument (Shimadzu, Kyoto, Japan) using a C18 column (5 μm × 250 nm × 4.6 nm, Elite Analytical Instruments Co., Ltd., Dalian, China) and equipped with a SPD-2A prominence UV/vis detector. Each sample (20 μL) was eluted at 30 °C with 0.01 M $(NH_4)H_2PO_4/CH_3OH$ = 13:7 (v/v, 1 mL/min) as the mobile phase, and absorbance at 228 nm was measured. The retention time for (*R*)-(−)-mandelic acid was 3.2 min. The optical purity of (*R*)-(−)-mandelic acid was determined by an analysis of the enantiomers on a CHIRALEL-OD-H column (250 × 4.6 mm) (Daicel Chemical Industries, Shinzaike, Japan) at a flow rate of 0.8 mL/min with a mobile phase containing hexane, 2-propanol, and trifluoroacetic acid (90:10:0.1, v/v) at a wavelength of 228 nm.

One unit of nitrilase activity was defined as the amount of enzyme that produces 1 μmol of (*R*)-(−)-mandelic acid per minute under the conditions described above. Protein quantitative analysis was conducted using the Bradford method[34] with bovine serum albumin as a standard.

Optimum pH and pH Stability. To investigate the optimal pH and the effect of pH on the activity of nitrilase, four buffers including citrate buffer (pH 3.0−6.0), phosphate buffer (pH 6.0−8.5), Tris-HCl buffer (pH 7.0−8.5), and glycine-NaOH buffer (pH 8.5−10.0) with a concentration of 100 mM were used, and the reactions were performed at 45 °C using 100 mM (*R*,*S*)-mandelonitrile as substrate. To investigate pH stability, the enzyme was dissolved in buffers of pHs ranging from 6.5 to 8.5 and incubated at 0 °C from 0.5 to 6 h, and then the relative activities were performed with standard assay conditions. Activity without treatment obtained at pH 8.0 was used as a blank and regarded as 100%.

Optimum Temperature and Thermal Stability. The optimal temperature of the enzyme was determined by assaying enzyme activities at temperatures ranging from 25 to 65 °C. Thermal stability was investigated by incubating enzymes at temperatures ranging from 30 to 60 °C. The enzyme was incubated in a heat-block at the specified temperature for a certain time. The relative activities were examined at 45 °C for 10 min.

Circular Dichroism (CD) Measurements. CD spectra were recorded on a JASCO J-815 Spectropolarimeter (JASCO Inc., Easton, MD) with Spectra Manager 228 software. The temperature was controlled from 10 to 60 °C using a Fisher Isotemp Model 3016S water bath (Fisher Scientific, Waltham, MA). A lyophilized powder (purity >95%, w/w) was prepared. A stock solution of 0.02 mg/mL nitrilase was generated in ddH_2O. The spectra were recorded from 190 to 250 nm.

Homology Modeling and Molecular Docking. The three-dimensional homology model of nitrilase was constructed using Build Homology Models (MODELER) in Discovery studio (DS) 2.1 (Accelrys Software, San Diego) and the crystal structure of a hypothetical protein PH0642 (PDB accession code 1J31) was used as the template. The catalytic tunnel size was analyzed using software HotSpot Wizard to identify the residues essential for protein function, enzyme activity, and substrate specificity. Autodock 4.0 was used to study the interaction between substrate and nitrilase, and to predict the spatial structure and catalytic mechanism of the nitrilase.

Time Course of (*R*,*S*)-Mandelonitrile Hydrolysis. The reaction mixture (10 mL) contained 0.1 g of wet cells of wild-type or evolved nitrilase suspended in 100 mM potassium phosphate buffer (pH 8.0) containing 100 mM (*R*,*S*)-mandelonitrile. These reactions were carried out at 40 °C in a reciprocal shaker at 150 rpm. Samples were removed at predetermined times, and the yield was determined by HPLC.

Fed-Batch Production of (*R*)-(−)-Mandelic Acid Using Mut3 as the Catalyst. The fed-batch reaction was performed at 40 °C and 150 rpm in 200 mL reaction volume. The reaction mixture contained 100 mM potassium phosphate buffer (pH 8.0), 100 mM (*R*,*S*)-mandelonitrile, and 5% wet cells of Mut3. (*R*,*S*)-mandelonitrile (100 mM) was fed in the subsequent 7 batches (total 800 mM) once an hour. The reaction mixture (100 μL) was periodically withdrawn and analyzed by HPLC.

Isolation and Identification of (*R*)-(−)-Mandelic Acid. The isolation procedure of (*R*)-(−)-mandelic acid was performed according to the following procedure: 2% (w/v) activated carbon was added into the fed-batch reaction mixture (200 mL) to remove the cells. After filtration, the filtrate adjusted to pH 9.0−10.0 with 2 M NaOH was extracted with an equal volume of ethyl acetate twice to obtain the aqueous phase, which was acidified to pH 1.0−2.0 with 2 M HCl. The aqueous phase suffered from vacuum filtration (SHB-III, Zhengzhou trade Co., LTD, China) to remove the proteins in the solvent, and then the filtrate was extracted with isopyknic ethyl acetate three times. After the organic extract was dried by anhydrous sodium sulfate, the solvent was removed through vacuum distillation (Adyantag ML, Heidolph, Germany) in a rotary evaporator, and the crystal of (*R*)-mandelic acid was subsequently obtained.

The ^{13}C and ^{1}H nuclear magnetic resonance (NMR) spectra of (*R*)-(−)-mandelic acid were obtained on a NMR spectrometer (AVANCE 500 MHz, Bruker, Fallanden, Switzerland) with DMSO as the solvent, using 500 and 125 MHz for carbon and proton determinations, respectively. The FTIR spectrum for (*R*)-(−)-mandelic acid was recorded on a Fourier transform infrared spectrometer (Nicolet 6700; Thermo, Waltham, MA) with a Contimμm FTIR Micro system in the region of 4000−400 cm^{-1} using KBr pellets. The LC-MS spectrum for (*R*)-mandelic acid was recorded on a high performance liquid chromatography−time-of-flight mass spectrometer (Agilent Technologies 1200 Series, 6210 Time-of-Flight MS spectrometer) (Agilent Technologies, Waldbronn, Germany), and the experimental parameters were used as follows: ionization mode, ESI scan; gas temperature, 300 °C; fragmentor, 80 V; drying gas, 3.5 L/min; skimmer, 65 V; nebulizer, 20 psig; OCTIRFV pp, 250 V; and Vcap, 3000 V.

Statistical Analysis. If not specifically noted, all experiments in this study were performed in triplicate. Analysis of variance (ANOVA) was carried out using the SAS program, version 8.1 (SAS Institute Inc., Cary, NC). Least significant differences (LSD) were computed at $P < 0.05$.

RESULTS

Construction and Screening of Mutant Libraries. The PCR products of GSSM were purified and digested by *Dpn* I to remove the template plasmid containing the methylation sites and to create the recombination library of pET28b-NIT_{mut}. Single colonies of positive mutants were picked from LB agar plates containing Kan resistance to 96-well plates with 200 μL of LB broth supplemented with 50 mg/mL of Kan and incubated overnight with vigorous shaking (500 rpm) at 37 °C. Ten microliters of the culture was transferred to the new 96-

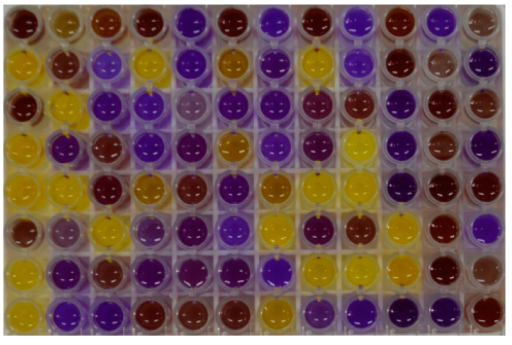

Figure 1. Mutant library screening for the high activity of nitrilases in a 96-well plate.

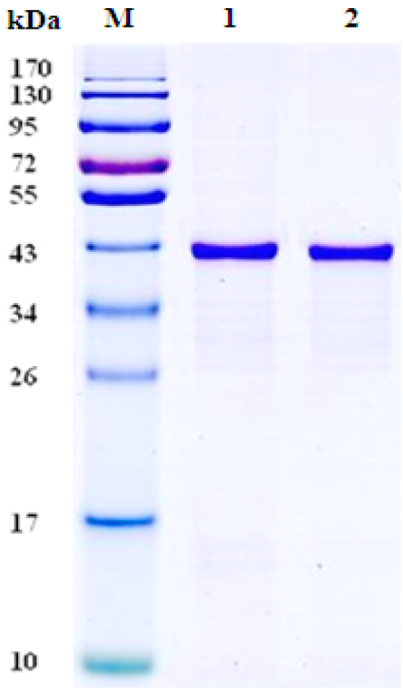

Figure 2. SDS−PAGE analysis of purified nitrilases. Gels with 30% polyacrylamide were subjected to protein analysis, and the protein bands were stained with Coomassie blue R250. Lanes 1 and 2 stand for Mut3 and the wild-type nitrilase, respectively.

well plates with 50 mg/mL Kan and 500 μL of LB medium, and then was incubated at 37 °C until the OD at 600 nm of the culture broth reached between 0.6 and 0.8 for retesting the activity and pH stability. In addition, plates containing both 100 mM (*R*,*S*)-mandelonitrile and 0.1 mM IPTG were incubated for 10 h at 28 °C. The final concentration of 0.01% (w/v) bromocresol purple solution was added for screening. The wells containing positive colonies with improved properties could become yellow and the negative mutants remain in the purple background (Figure 1 and Figure S1 in the Supporting Information). Over 6300 colonies in total were screened, and 55 clones could make the wells turn yellow. Among these clones, 10 better ones were retested using HPLC, and the clone with the greatest improvement in activity was selected (Table S1 in the Supporting Information). At the same time, selected variants were sequenced, and their amino acid substitutions are listed in Table S1 (Supporting Information). After three rounds of GSSM followed by screening, a best mutant Mut3 (Gln196Ser/Ala284Ile), with 200% relative activity than the wild-type, was selected as the targeted evolved nitrilase for further studies.

Expression and Purification of Nitrilases. The wild-type and evolved nitrilases were subjected to Nickel-NTA affinity chromatography. As shown in SDS−PAGE (Figure 2), there is only one pure band with a molecular weight of around 43 kDa observed for both of the purified wild-type and evolved nitrilases, which is consistent with the predicted molecular weight.

Influences of pH Values on the Activites of Nitrilases. It is well-known that the pH values affect the ionic environment of the enzyme, thus acting on its interaction between substrate and enzyme activity. To investigate the effect of pH on nitrilase activity, the reaction was performed in buffers including citrate buffer (pH 3.0−6.0), phosphate buffer (pH 6.0−8.5), Tris-HCl buffer (pH 7.0−8.5), and glycine-NaOH buffer (pH 8.5−10.0) with a concentration of 100 mM at 45 °C. As shown in Figure 3A, both wild-type nitrilase and Mut3 showed almost the same trends of activities under different pH conditions. The maximum specific activity of the evolved and wild-type nitrilases was observed at pH 8.0. Compared to wild-type nitrilase, the activity of Mut3 has increased significantly ranging from pH 3.0 to 10.0. Moreover, at pH 8.0, the specific activity of Mut3 (42.77 U/mg) was improved 154% compared to that of wild-type nitrilase (27.79 U/mg).

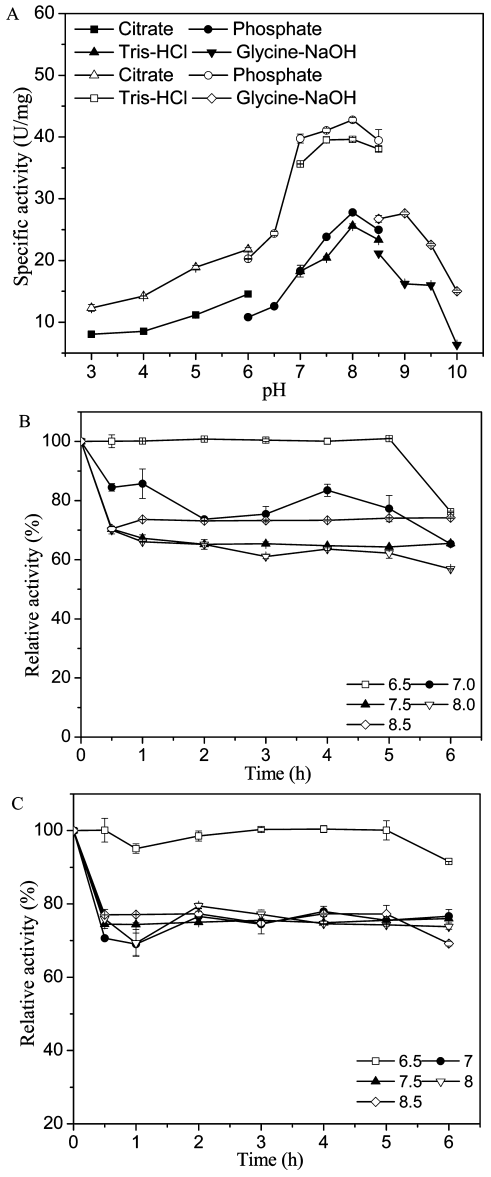

Figure 3. Influence of pH on the activity of nitrilases and stability. (A) Reactions were performed at 45 °C with different buffers. Hollow and solid represent the mutant Mut3 and the wild-type nitrilase, respectively. (B) pH stability was investigated by dissolving the wild-type nitrilase in phosphate buffers of pHs ranging from 6.5 to 8.5 and incubated at 0 °C from 0.5 to 6 h. (C) pH stability was investigated by dissolving Mut3 in phosphate buffers of pHs ranging from 6.5 to 8.5 and incubated at 0 °C from 0.5 to 6 h.

The pH stability study (Figure 3B and C) showed that Mut3 was more stable at pH 6.5 with about 90% residual activity after 6 h than the wild-type nitrilase with only 76% residual activity.

dx.doi.org/10.1021/jf405683f | J. Agric. Food Chem. 2014, 62, 4685−4694

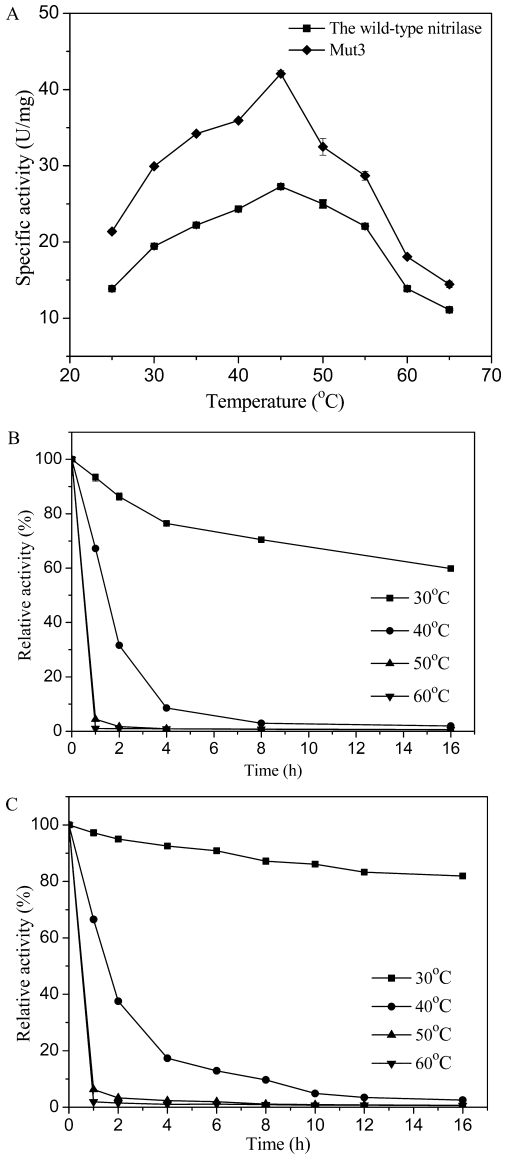

Figure 4. Effect of temperature on the activity of nitrilases and stability. (A) Reactions were performed in 100 mM at pH 8.0 phosphate buffer at various temperatures ranging from 25 to 65 °C. (B) Thermal stability was investigated by incubating the wild-type nitrilase at temperatures ranging from 30 to 60 °C. (C) Thermal stability was investigated by incubating Mut3 at temperatures ranging from 30 to 60 °C.

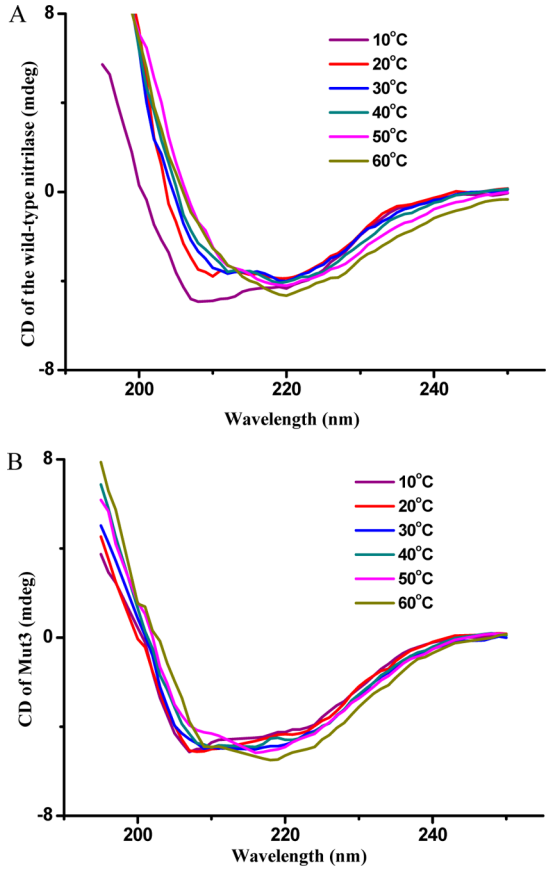

Figure 5. spectroscopic structural analyses of nitrilases. CD wavelength scans of the wild-type nitrilase (A) and Mut3 (B) at pH 7.5.

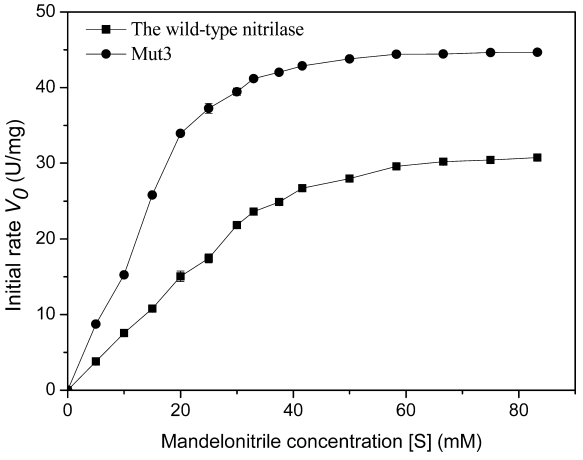

Figure 6. Reaction rate at different mandelonitrile concentrations. Reactions were performed at 45 °C, 150 rpm, with 100 mM potassium phosphate buffer (pH 8.0).

Effects of Temperatures on the Activities. The effects of temperatures on nitrilase activities of the wild-type and Mut3 were investigated. Enzyme (0.2 mg/mL) was dissolved in 100 mM phosphate buffer (pH 8.0) and incubated for 5 min at a temperature ranging from 25 to 65 °C before reaction. The reaction was started by adding 100 mM (*R*,*S*)-mandelonitrile under the corresponding temperature at 150 rpm for 10 min in a reciprocal shaker. As shown in Figure 4A, the optimum temperatures were 45 °C for both the wild-type and Mut3. The activities of nitrilases decreased significantly when the temperature was above 45 °C, and the specific activity of Mut3 was about 154% higher as compared to the wild-type nitrilase under the optimal temperature and pH.

The study of thermostability showed that the activity of wild-type nitrilase maintained about 60% incubation after 16 h, while the residual activity of Mut3 was 75% at 30 °C. After incubation for 1 h at 50 and 60 °C, the relative activity of wild-type nitrilase was sharply reduced to 4.40% and 1.03%, and Mut3 was 6.30% and 1.92%, respectively. Mut3 was unstable at higher temperature as revealed by a half-life of 54 h at 30 °C, 1.9 h at 40 °C, and 0.4 h at 50 °C, which was better than that of the wild-type nitrilase with half-lives of 21 h at 30 °C, 1.8 h at 40 °C, and 0.2 h at 50 °C (Figure 4B and C). The results corresponded to the circular dichroism data, indicating the

dx.doi.org/10.1021/jf405683f | J. Agric. Food Chem. 2014, 62, 4685−4694

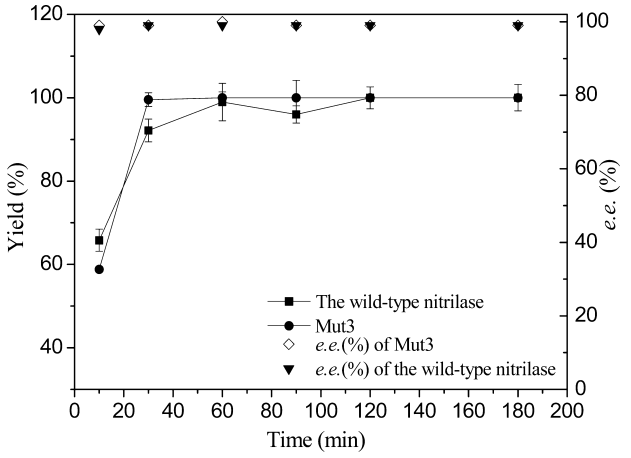

Figure 7. Time course analysis of (*R*,*S*)-mandelonitrile biotransformation by wild-type nitrilase and Mut3 under optimal conditions with a pH of 8.0, a temperature of 40 °C, and a concentration of (*R*,*S*)-mandelonitrile of 100 mM.

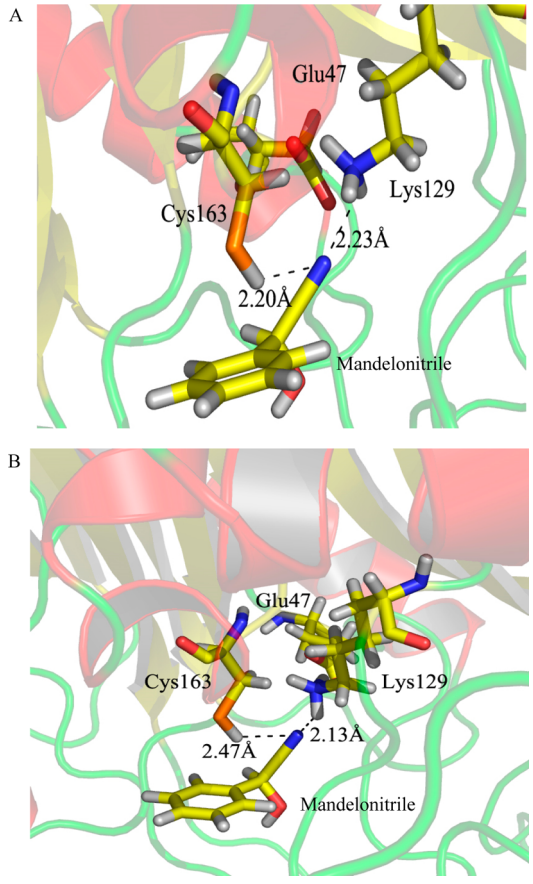

Figure 8. Homology modeling and docking analysis of nitrilases with mandelonitrile docking into the active site of the wild-type nitrilase (A) and Mut3 (B).

nitrilases were sensitive to heat (Figure 5 and Table S2, Supporting Information).

Kinetic Analysis of Wild-Type and Evolved Nitrilase. To determine the kinetics of reaction catalyzed by nitrilases, the initial rate V_0 was investigated at different concentrations (0–100 mM) of (*R*,*S*)-mandelonitrile (Figure 6). The experimental data were fitted to the Michaelis–Menten equation ($V_0 = (V_{max}[S])/(K_m + [S])$), and the values of K_m and V_{max} were

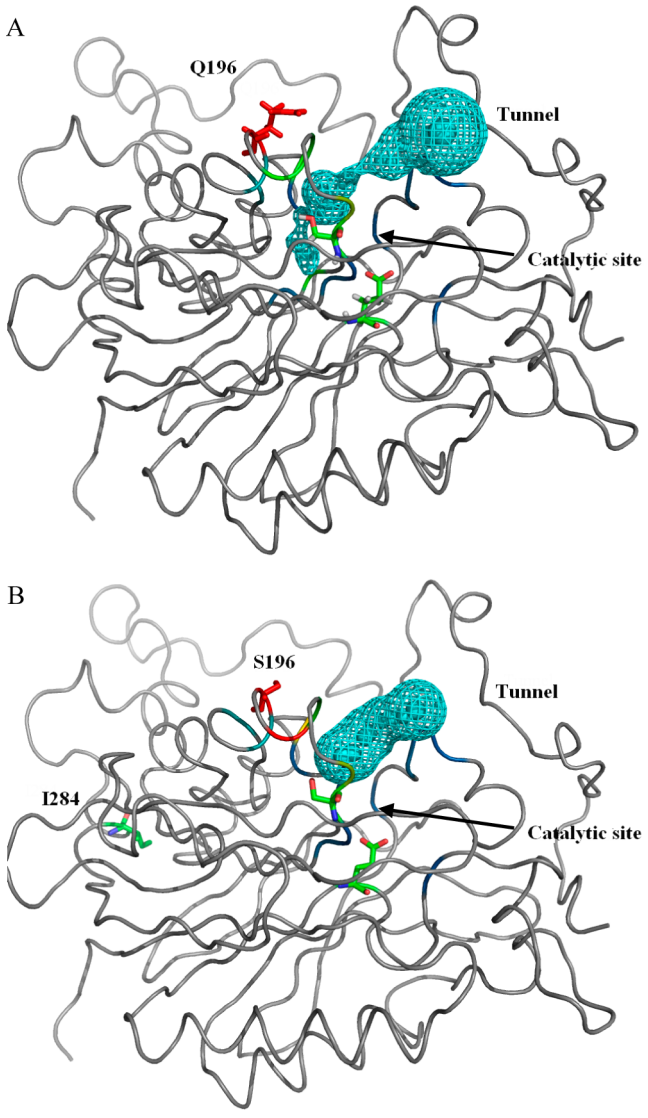

Figure 9. Tunnel analyses of wild-type nitrilase (A) and Mut3 (B).

calculated according to the Lineweaver–Burk plots. The values of K_m, V_{max}, and k_{cat} were calculated to be 20.64 mM, 33.74 μmol mg^{-1} min^{-1}, and 24.45 s^{-1} for wild-type nitrilase, while they were 9.24 mM, 47.68 μmol mg^{-1} min^{-1}, and 34.55 s^{-1} for Mut3, respectively.

Time Course of (*R*,*S*)-Mandelonitrile Hydrolysis. Wet cells of wild-type or Mut3 (0.1 g) was suspended in the 10 mL reaction mixture containing 100 mM potassium phosphate buffer (pH 8.0) and 100 mM (*R*,*S*)-mandelonitrile. The reactions were carried out at 40 °C in a reciprocal shaker at 150 rpm. Samples were removed at predetermined times, and the yield was determined by HPLC analysis. As shown in Figure 7, the yield of Mut3 could reach 100% in 0.5 h which was higher than that of the wild-type, and the enantiomeric excess (e.e.) of (*R*)-(−)-mandelic acid was >99%.

Fed-Batch Production of (*R*)-(−)-Mandelic Acid. To obtain efficient production of (*R*)-(−)-mandelic acid and reduce the potential inhibition on enzyme at high substrate concentration, a fed-batch reaction was performed using Mut3 as catalyst. (*R*,*S*)-Mandelonitrile (100 mM) was fed to the subsequent 7 batches (total concentration of substrate: 800 mM) once an hour. The accumulative concentration of (*R*)-

dx.doi.org/10.1021/jf405683f | J. Agric. Food Chem. 2014, 62, 4685–4694

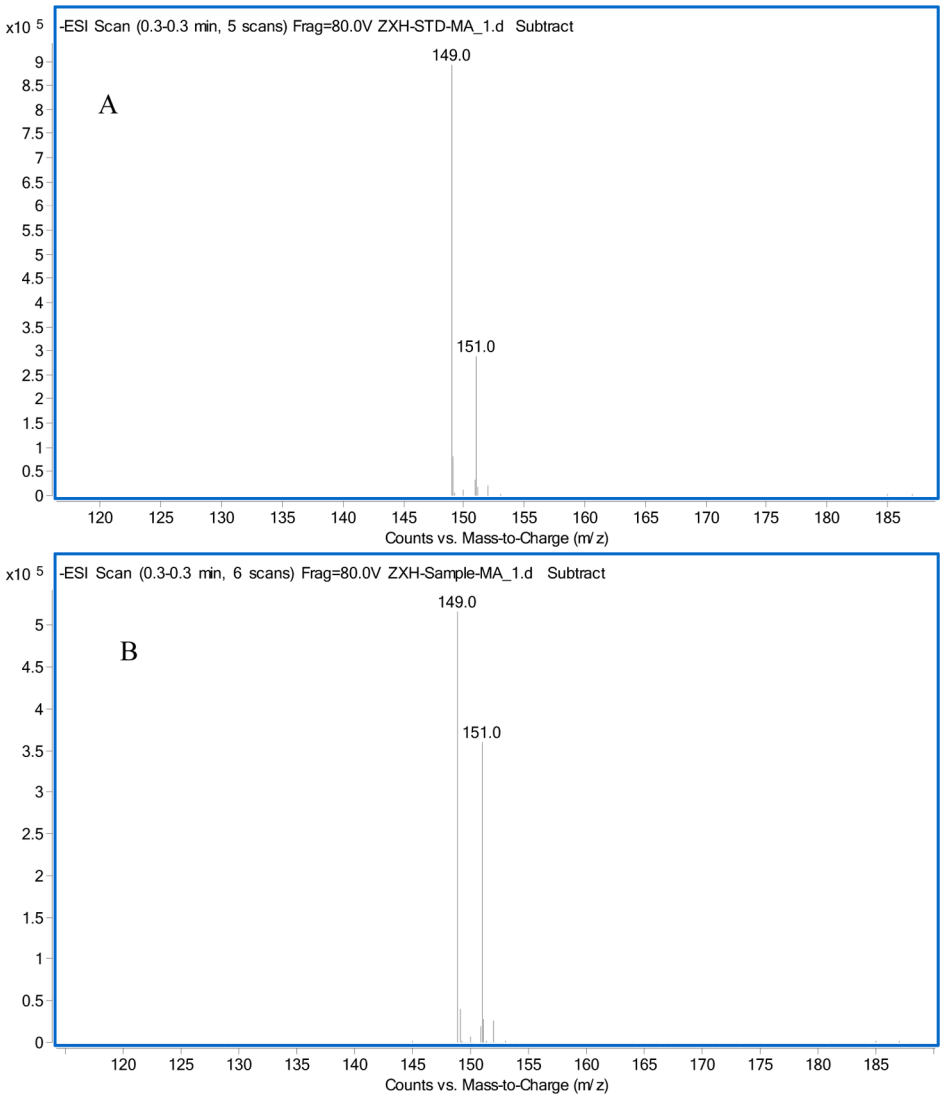

Figure 10. Identification of (*R*)-(−)-mandelic acid. LC-MS spectrum of (*R*)-(−)-mandelic acid, standard (*R*)-(−)-mandelic acid (A), and separated (*R*)-(−)-mandelic acid (B).

(−)-mandelic acid reached 585 mM after 5.5 h of biotransformation (Figure S2, Supporting Information). Compared to the previous report,[35] 693 mM of (*R*)-(−)-mandelic acid concentration at 7.5 h in this work displayed the highest productivity in terms of the nitrilase catalyzing asymmetric hydrolysis of (*R,S*)-mandelonitrile, and the optical purity of the (*R*)-(−)-mandelic acid was maintained above 99% during the reaction process. In addition, considering the cost of industrial application, Mut3 with excellent tolerance against high product concentration is more favorable for applications because the separation cost of product will be reduced substantially. Taking the volumetric productivity and product concentration tolerance into account, the mutant Mut3 was potential for industrial application.

Isolation and Identification of (*R*)-Mandelic Acid. After isolation and purification of (*R*)-(−)-mandelic acid according to the method described in Materials and Methods, (*R*)-(−)-mandelic acid with 99% purity was obtained (Figure S3, Supporting Information). The LC-MS spectrum of the separated (*R*)-(−)-mandelic acid was presented in Figure 10A and B, LC-MS showed that the molecular ion peak of (*R*)-(−)-mandelic acid was *m/z* 151.0, which was in accordance with the mass of (*R*)-(−)-mandelic acid. The FTIR spectrum of the separated (*R*)-(−)-mandelic acid is presented in Figure 11A and B; the two sharp peaks presented at 3448 and 1724 cm^{-1} could be assigned to the O−H and C═O stretching vibrations, respectively. The two peak absorption bands at 1495 and 1455 cm^{-1} were due to the C═C stretching vibration on the phenyl group. When ^{13}C NMR was performed, the isolated product gave one signal at 174 ppm, which referred to the C positions of the carboxyl group. The absorption bands between 126 and 140 ppm were due to the C positions on the phenyl group (Figure S4, A and B, Supporting Information). Figure S5, A and B (Supporting Information) shows four different kinds of H atoms, which corresponded to the structure of (*R*)-(−)-mandelic acid, one peak at chemical shift δ = 12.6356 ppm representing one H atom at the carboxyl group. The split peaks at chemical shifts between δ = 7.2797 ppm and δ = 7.4522 ppm represented the H positions on the phenyl group, and the peak at chemical shift δ = 2.50 ppm referred to the H position of the hydroxyl group. Accordingly, it was concluded that the isolated product was (*R*)-(−)-mandelic acid.

dx.doi.org/10.1021/jf405683f | J. Agric. Food Chem. 2014, 62, 4685−4694

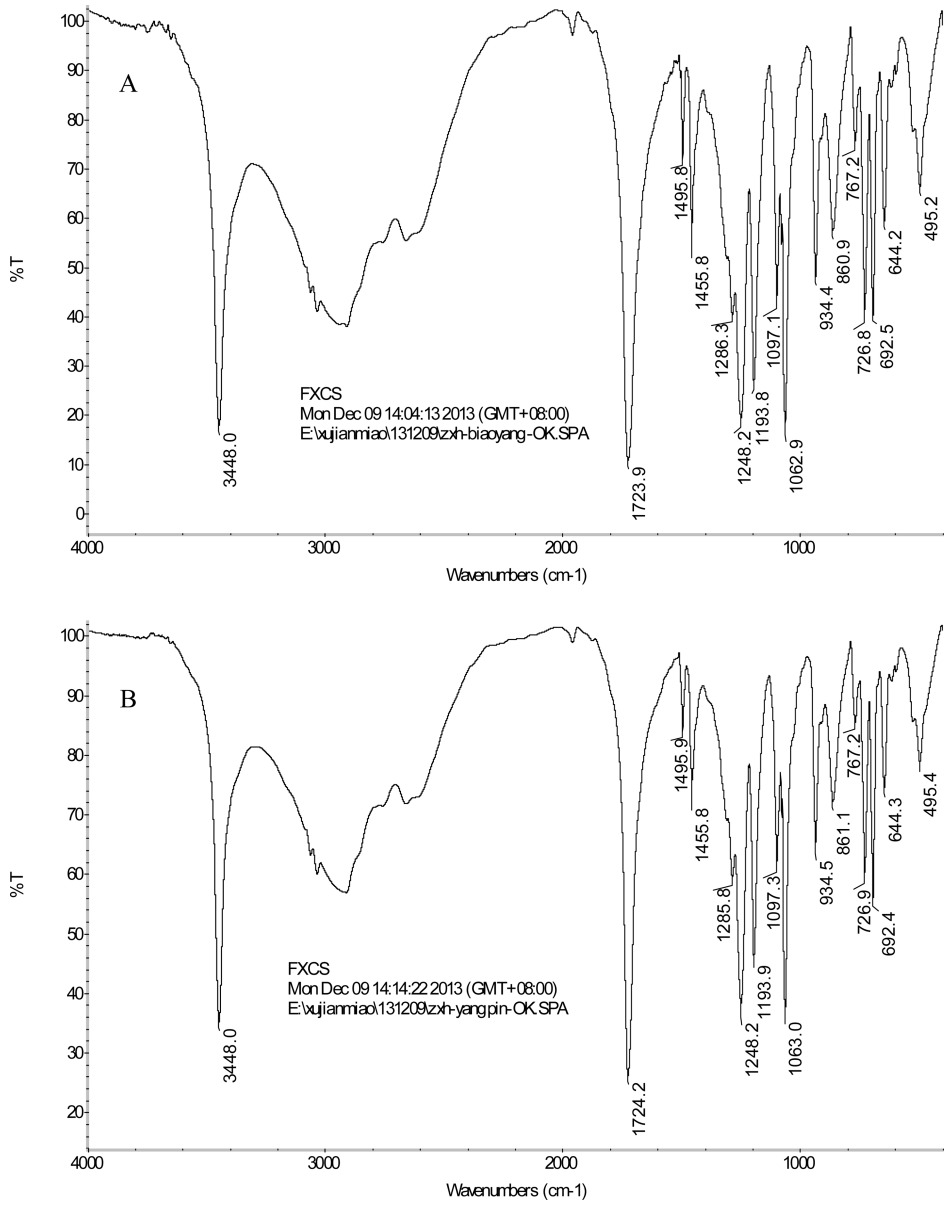

Figure 11. Identification of (*R*)-(−)-mandelic acid. Infrared spectroscopy of (*R*)-(−)-mandelic acid, standard (*R*)-(−)-mandelic acid (A), and separated (*R*)-mandelic acid (B).

Table 2. Comparison of Wild-Type Nitrilase and Mut3 with Reported Nitrilases

substrate (mM)	bacteria	resting cells (g)	reaction time (h)	the volume of reaction (mL)	yield (%)	reference
100	*E. coli* JM109/pNLE	0.01	2	1	100	15
100	*E. coli* M15/BCJ2315	0.1	1	10	99.1	37
100	the wild-type nitrilase	0.1	1	10	100	this work
100	Mut3	0.1	0.5	10	100	this work

DISCUSSION

Nitrilases have recently drawn considerable attention due to their ability to transform nitriles to carboxylic acids with chemo-, region-, and enantioselectivity.[36,37] Nitrilases, as important industrial enzymes, have more significant improvements than traditional chemical catalysts,[38] which have mediated the industrial conversion of aliphatic, arylaliphatic, aromatic, and heterocyclic nitriles.[6,37] One of the important industrial applications of nitrilases is the conversion of (*R*,*S*)-mandelonitrile to (*R*)-(−)-mandelic acid with high enantioselectivity, low cost, and almost 100% yield.[5,11,12] The goal of this study is to improve the nitrilase from *A. faecalis* to meet the requirement of an upscale production of (*R*)-(−)-mandelic acid.

On the basis of the secondary structure, relationships between substrate and the nitrilase, and previous reports,[5,31,32] five sites (Leu175, Ala197, Val305, Ala284, and Gln196) were selected to carry out mutations for improving activity of nitrilase. After screening by a two step screening method, the best mutant Mut3 was selected. Mut3 displayed dramatic improvement in activity, pH stability, and tolerance to the

dx.doi.org/10.1021/jf405683f | J. Agric. Food Chem. 2014, 62, 4685−4694

substrate. In a fed-batch reaction with 800 mM (*R,S*)-mandelonitrile as the substrate, the cumulative concentration of (*R*)-(−)-mandelic acid in the reaction mixture after 5.5 h of biotransformation reached 585 mM with an e.e. of 99%, which was higher than that in a previous report with 520 mM after 18 h. At the same time, the space-time productivity of Mut3 (10.64 mmol L^{-1} h^{-1} g^{-1}) was 7.40-fold higher than that in a previous report (1.44 mmol L^{-1} h^{-1} g^{-1}).[35]

CD results confirmed that these nitrilases are sensitive to heat and that the thermostability of Mut3 was better than that of wild-type nitrilase. The nitrilase activites of both wild-type and Mut3 shared almost the same trends under different pH conditions. The specific activity of Mut3 (42.77 U/mg) was 154% higher than that of wild-type nitrilase (27.79 U/mg) at pH 8.0. The analysis of the time course of (*R,S*)-mandelonitrile hydrolysis indicated that the yield of Mut3 could reach 100% in 0.5 h, which was shorter than that of wild-type nitrilase with 1 h. Especially, the time-space productivity of (*R*)-(−)-mandelic acid by Mut3 was superior to those in previous reports (Table 2).[35,39]

Homology modeling and molecular docking analysis can predict spatial structure and the catalytic mechanism of nitrilase (Figure 8). Modeling and mutation studies showed that conserved catalytic residues Cys163, Glu47, and Lys129 are the catalytic triad of the nitrilase. Cys163 attacks cyano as affinity reagents with hydrogen bonds, Lys129 has a stabilizing effect on the triplet complex with hydrogen bonds, and Glu47 plays a leading role in catalysis.[5] The tunnel analysis indicated that the diameter of the catalytic tunnel and tunnel volume for Mut3 were 1.70 and 16.0 $Å^3$ compared with 0.43 and 23.0 $Å^3$ for the wild-type (Figure 9). The larger catalytic tunnel and smaller tunnel volume can improve the nitrilase to hold and selectively catalyze the substrate.[30,32]

In summary, we genetically engineered the nitrilase originated from *A. faecalis* nitrilase by GSSM for the production of (*R*)-(−)-mandelic acid. A mutant, Mut3 with high activity, enantioselectivity, and stability in high concentrations of substrate or product, had been obtained. The thermostability of Mut3 was better than that of wild-type nitrilase. After mutation, Mut3 achieved the highest space-time productivity (10.64 mmol L^{-1} h^{-1} g^{-1}). The results in this work indicated that Mut3 was a promising biocatalyst for the production of (*R*)-(−)-mandelic acid in industrial applications. This study paved a foundation for the large-scale biotransformation of (*R,S*)-mandelonitrile to (*R*)-(−)-mandelic acid. Further studies will focus on the upscale production of (*R*)-(−)-mandelic acid using Mut3 as the biocatalyst and are underway in our laboratory.

■ ASSOCIATED CONTENT

Supporting Information

Relative activities of wild-type and evolved nitrilases, comparison of θ208, θ222, and θ216 at different temperatures of nitirilases, color images of bromocresol purple responding to increasing mandelic acid concentration, time-course profile for the preparation of (*R*)-(−)-mandelic acid which was fed in the subsequent 7 feeds (total 800 mM), crystal of (*R*)-(−)-mandelic acid, and ^1H and ^{13}C NMR of (*R*)-(−)-mandelic acid. This material is available free of charge via the Internet at http://pubs.acs.org.

■ AUTHOR INFORMATION

Corresponding Author

*Tel: +86-571-88320630. Fax: +86-571-88320630. E-mail: zhengyg@zjut.edu.cn.

Funding

This work was financially supported by the National High Technology Research and Development Program of China (863 Program) (No. 2011AA02A210), Natural Science Foundation of Zhejiang Province (No. R3110155, Z4090612 and Y4110409), and Qianjiang Talent Project of Zhejiang Province.

Notes

The authors declare no competing financial interest.

■ REFERENCES

(1) Kirk, O.; Borchert, T. V.; Fuglsang, C. C. Industrial enzyme applications. *Curr. Opin. Biotechnol.* **2002**, *13* (4), 345−351.

(2) Straathof, A. J.; Panke, S.; Schmid, A. The production of fine chemicals by biotransformations. *Curr. Opin. Biotechnol.* **2002**, *13* (6), 548−556.

(3) Gong, J. S.; Lu, Z. M.; Li, H.; Shi, J. S.; Zhou, Z. M.; Xu, Z. H. Nitrilases in nitrile biocatalysis: recent progress and forthcoming research. *Microb. Cell Fact.* **2012**, *11* (1), 142.

(4) Liu, Z. Q.; Baker, P. J.; C, F.; Xue, Y. P.; Zheng, Y. G.; Shen, Y. C. Screening and improving the recombinant nitrilases and application in biotransformation of iminodiacetonitrile to iminodiacetic acid. *PLoS One* **2013**, *8* (6), e67197.

(5) Liu, Z. Q.; Dong, L. Z.; Cheng, F.; Xue, Y. P.; Wang, Y. S.; Ding, J. N.; Zheng, Y. G.; Shen, Y. C. Gene cloning, expression, and characterization of a nitrilase from *Alcaligenes faecalis* ZJUTB10. *J. Agric. Food. Chem.* **2011**, *59* (21), 11560−11570.

(6) O'Reilly, C.; Turner, P. D. The nitrilase family of CN hydrolysing enzymes - a comparative study. *J. Appl. Microbiol.* **2003**, *95* (6), 1161−1174.

(7) Kaul, P.; Banerjee, A.; Mayilraj, S.; Banerjee, U. C. Screening for enantioselective nitrilases: kinetic resolution of racemic mandelonitrile to (*R*)-(−)-mandelic acid by new bacterial isolates. *Tetrahedron: Asymmetry* **2004**, *15* (2), 207−211.

(8) Rustler, S.; Muller, A.; Windeisen, V.; Chmura, A.; Fernandes, B. C. M.; Kiziak, C.; Stolz, A. Conversion of mandelonitrile and phenylglycinenitrile by recombinant *E. coli* cells synthesizing a nitrilase from *Pseudomonas fluorescens* EBC191. *Enzyme Microb. Technol.* **2007**, *40* (4), 598−606.

(9) Zhang, H. J.; Q, W.; Zhou, Q. W.; Zhou, G. C. Biotransformation of the neonicotinoid insecticide thiacloprid by the *Bacterium Variovorax* boronicumulans strain J1 and mediation of the major metabolic pathway by nitrile hydratase. *J. Agric. Food. Chem.* **2012**, *60* (1), 153−159.

(10) Mullaney, J. A.; Kelly, W. J.; Mcghie, T. K. Lactic acid bacteria convert glucosinolates to nitriles efficiently yet differently from enterobacteriaceae. *J. Agric. Food. Chem.* **2013**, *61* (12), 3039−3046.

(11) Xue, Y. P.; Liu, Z. Q.; Xu, M.; Wang, Y. J.; Zheng, Y. G.; Shen, Y. C. Enhanced biotransformation of (*R,S*)-mandelonitrile to (*R*)-(−)-mandelic acid with in situ production removal by addition of resin. *Biochem. Eng. J.* **2010**, *53* (1), 143−149.

(12) Xiao, M. T.; Huang, Y. Y.; Ye, J.; Guo, Y. H. Study on the kinetic characteristics of the asymmetric production of *R*-(−)-mandelic acid with immobilized *Saccharomyces cerevisiae* FD11b. *Biochem. Eng. J.* **2008**, *39* (2), 311−318.

(13) Tang, K.; Yi, J.; Huang, K.; Zhang, G. Biphasic recognition chiral extraction: A novel method for separation of mandelic acid enantiomers. *Chirality* **2009**, *21* (3), 390−395.

(14) Xue, Y. P.; Xu, S. Z.; Liu, Z. Q.; Zheng, Y. G.; Shen, Y. C. Enantioselective biocatalytic hydrolysis of (R,S)-mandelonitrile for production of (R)-(-)-mandelic acid by a newly isolated mutant strain. *J. Ind. Microbiol. Biotechnol.* **2011**, *38* (2), 337−345.

(15) Schmid, A.; Dordick, J. S.; Hauer, B.; Kiener, A.; Wubbolts, M.; Witholt, B. Industrial biocatalysis today and tomorrow. *Nature* **2001**, *409* (6817), 258−268.
(16) Takahashi, E.; Nakamichi, K.; Furui, M.; Mori, T. *R*-(−)-Mandelic acid production from racemic mandelic acids by *Pseudomonas polycolor* with asymmetric degrading activity. *J. Ferment. Bioeng.* **1995**, *79* (5), 439−442.
(17) Williams, D. J.; Critchley, C.; Pun, S.; Chaliha, M. Key role of Fe^{2+} in epithiospecifier protein activity. *J. Agric. Food. Chem.* **2010**, *85* (15), 8512−8521.
(18) He, Y. C.; Xu, J. H.; Xu, Y.; Ouyang, L. M.; Pan, J. Biocatalytic synthesis of R-(-)-mandelic acid from racemic mandelonitrile by a newly isolated nitrilase-producer *Alcaligenes* sp. ECU0401. *Chinese Chem. Lett.* **2007**, *18* (6), 677−680.
(19) Naik, S. C.; Kaul, P.; Barse, B.; Banerjee, A.; Banerjee, U. C. Studies on the production of enantioselective nitrilase in a stirred tank bioreactor by *Pseudomonas putida* MTCC 5110. *Bioresour. Technol.* **2008**, *99* (1), 26−31.
(20) Yamamoto, K.; Oishi, K.; Fujimatsu, I.; Komatsu, K. Production of *R*-(−)-mandelic acid from mandelonitrile by *Alcaligenes faecalis* ATCC 8750. *Appl. Environ. Microbiol.* **1991**, *57* (10), 3028−3032.
(21) Nagasawa, T.; Mauger, J.; Yamada, H. A novel nitrilase, arylacetonitrilase, of *Alcaligenes faecalis* JM3 - purification and characterization. *Eur. J. Biochem.* **1990**, *194* (3), 765−772.
(22) Zhu, D. M.; Mukherjee, C.; Biehl, E. R.; Hua, L. Discovery of a mandelonitrile hydrolase from *Bradyrhizobium japonicum* USDA110 by rational genome mining. *Biochem. J.* **2007**, *129* (4), 645−650.
(23) Wang, H. L.; Sun, H. H.; Wei, D. Z. Discovery and characterization of a highly effcient enantioselective mandelonitrile hydrolase from *Burkholderia cenocepacia* J2315 by phylogeny-based enzymatic substrate specificity prediction. *BMC Biotechnol.* **2013**, *13*, 14.
(24) Liu, Z. Q.; Sun, Z. H.; Leng, Y. Directed evolution and characterization of a novel D-pantonohydrolase from *Fusarium moniliforme*. *J. Agric. Food. Chem.* **2006**, *54* (16), 5823−5830.
(25) Zoller, M. J.; Smith, M. Oligonucleotide-directed mutagenesis using M13-derived vectors: an efficient and general procedure for the production of point mutations in any fragment of DNA. *Nucleic Acids Res.* **1982**, *10* (20), 6487−6500.
(26) Yeom, S. J.; Lee, J. K.; Oh, D. K. A positively charged amino acid at position 129 in nitrilase from *Rhodococcus rhodochrous* ATCC 33278 is an essential residue for the activity with meta-substituted benzonitriles. *FEBS Lett.* **2010**, *584* (1), 106−110.
(27) Wu, S. J.; Fogiel, A. J.; Petrillo, K. L.; Hann, E. C.; Mersinger, L. J.; DiCosimo, R.; O'Keefe, D. P.; Ben-Bassat, A.; Payne, M. S. Protein engineering of *Acidovorax facilis* 72W nitrilase for bioprocess development. *Biotechnol. Bioeng.* **2007**, *97* (4), 689−693.
(28) Wu, S. J.; Fogiel, A. J.; Petrillo, K. L.; Jackson, R. E.; Parker, K. N.; DiCosimo, R.; Ben-Bassat, A.; O'Keefe, D. P.; Payne, M. S. Protein engineering of nitrilase for chemoenzymatic production of glycolic acid. *Biotechnol. Bioeng.* **2008**, *99* (3), 717−720.
(29) Nolan, L. M.; Harnedy, P. A.; Turner, P.; Hearne, A. B.; O'Reilly, C. The cyanide hydratase enzyme of *Fusarium lateritium* also has nitrilase activity. *FEMS Microbiol. Lett.* **2003**, *221* (2), 161−165.
(30) Watanabe, A.; Yano, K.; Ikebukuro, K.; Karube, I. Investigation of the potential active site of a cyanide dihydratase using site-directed mutagenesis. *Biochim. Biophys. Acta* **1998**, *1382* (1), 1−4.
(31) Schreiner, U.; Hecher, B.; Obrowsky, S.; Waich, K.; Klempier, N.; Steinkellner, G.; Gruber, K.; Rozzell, J. D.; Glieder, A.; Winkler, M. Directed evolution of *Alcaligenes faecalis* nitrilase. *Enzyme Microb. Technol.* **2010**, *47* (4), 140−146.
(32) Williamson, D. S.; Dent, K. C.; Weber, B. W.; Varsani, A.; Frederick, J.; Thuku, R. N.; Cameron, R. A.; van Heerden, J. H.; Cowan, D. A.; Sewell, B. T. Structural and biochemical characterization of a nitrilase from the thermophilic bacterium, *Geobacillus pallidus* RAPc8. *Appl. Microbiol. Biotechnol.* **2010**, *88* (1), 143−153.
(33) Chung, C. T.; Niemela, S. L.; Miller, R. H. One-step preparation of competent *Escherichia coli*: transformation and storage of bacterial cells in the same solution. *Proc. Natl. Acad. Sci. U.S.A.* **1989**, *86* (7), 2172−2175.
(34) Bradford, M. M. A rapid and sensitive method for the quantitation of microgram quantities of protein utilizing the principle of protein-dye binding. *Anal. Biochem.* **1976**, *72* (1−2), 248−254.
(35) Zhang, Z. J.; Xu, J. H.; He, Y. C.; Ouyang, L. M.; Liu, Y. Y.; Imanaka, T. Efficient production of (*R*)-(−)-mandelic acid with highly substrate/product tolerant and enantioselective nitrilase of recombinant *Alcaligenes sp. Process Biochem.* **2010**, *45* (6), 887−891.
(36) Wang, M. X. Enantioselective biotransformations of nitriles in organic synthesis. *Top. Catal.* **2005**, *35* (1−2), 117−130.
(37) Thuku, R. N.; Brady, D.; Benedik, M. J.; Sewell, B. T. Microbial nitrilases: versatile, spiral forming, industrial enzymes. *J. Appl. Microbiol.* **2009**, *106* (3), 703−727.
(38) Martinkova, L.; Kren, V. Biotransformations with nitrilases. *Curr. Opin. Chem. Biol.* **2010**, *14* (2), 130−137.
(39) Ni, K. F.; Wang, H. L.; Zhao, L.; Zhang, M. J.; Zhang, S. Y.; Ren, Y. H.; Wei, D. Z. Efficient production of (*R*)-(−)-mandelic acid in biphasic system by immobilized recombinant *E.coli*. *J. Biotechnol.* **2013**, *167* (4), 433−440.